Supplementary Materials

Contrasting behaviors of the atmospheric CO_2 interannual variability during two types of El Niños

Jun Wang[1,2], Ning Zeng[2,3], Meirong Wang[4], Fei Jiang[1], Jingming Chen[1,5], Pierre Friedlingstein[6], Atul K. Jain[7], Ziqiang Jiang[1], Weimin Ju[1], Sebastian Lienert[8,9], Julia Nabel[10], Stephen Sitch[11], Nicolas Viovy[12], Hengmao Wang[1], Andrew J. Wiltshire[13]

[1]International Institute for Earth System Science, Nanjing University, Nanjing, China

[2] State Key Laboratory of Numerical Modelling for Atmospheric Sciences and Geophysical Fluid Dynamics, Institute of Atmospheric Physics, Beijing, China

[3]Department of Atmospheric and Oceanic Science and Earth System Science Interdisciplinary Center, University of Maryland, College Park, Maryland, USA

[4]Joint Center for Data Assimilation Research and Applications/Key Laboratory of Meteorological Disaster of Ministry of Education, Nanjing University of Information Science & Technology, Nanjing, China

[5]Department of Geography, University of Toronto, Ontario M5S3G3, Canada

[6]College of Engineering, Mathematics and Physical Sciences, Unvernity of Exeter, Exeter EX4 4QE, UK

[7]Department of Atmosheric Sciences, University of Illinois at Urbana-Champaign, Urbana, IL 61801, USA

[8]Climate and Environmental Physics, Physics Institute, University of Bern, Bern, Switzerland

[9]Oeschger Centre for Climate Change Research, University of Bern, Bern, Switzerland

[10]Land in the Earth System, Max Planck Institute for Meteorology, D-20146 Hamburg, Germany

[11]College of Life and Environmental Sciences, University of Exeter EX4 4QF, UK

[12]Laboratoire des Sciences du Climat et de l'Environnement, LSCE/IPSL-CEA-CNRS-UVQS, F-91191, Gif sur Yvette, France

[13]Met office Hadley Centre, Fitzroy Rd, Exeter. EX1 3PB. UK

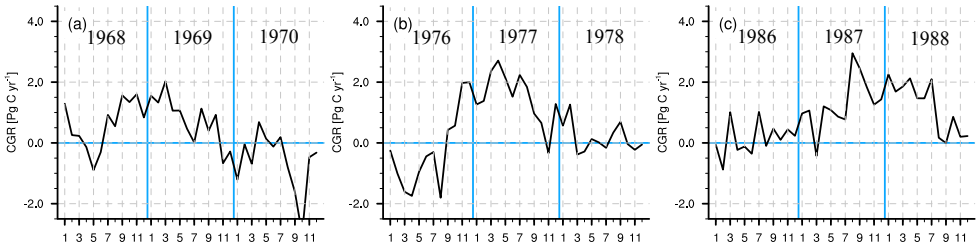

Figure S1 The atmospheric CO_2 growth rate anomalies in the long-lasting El Niño events.

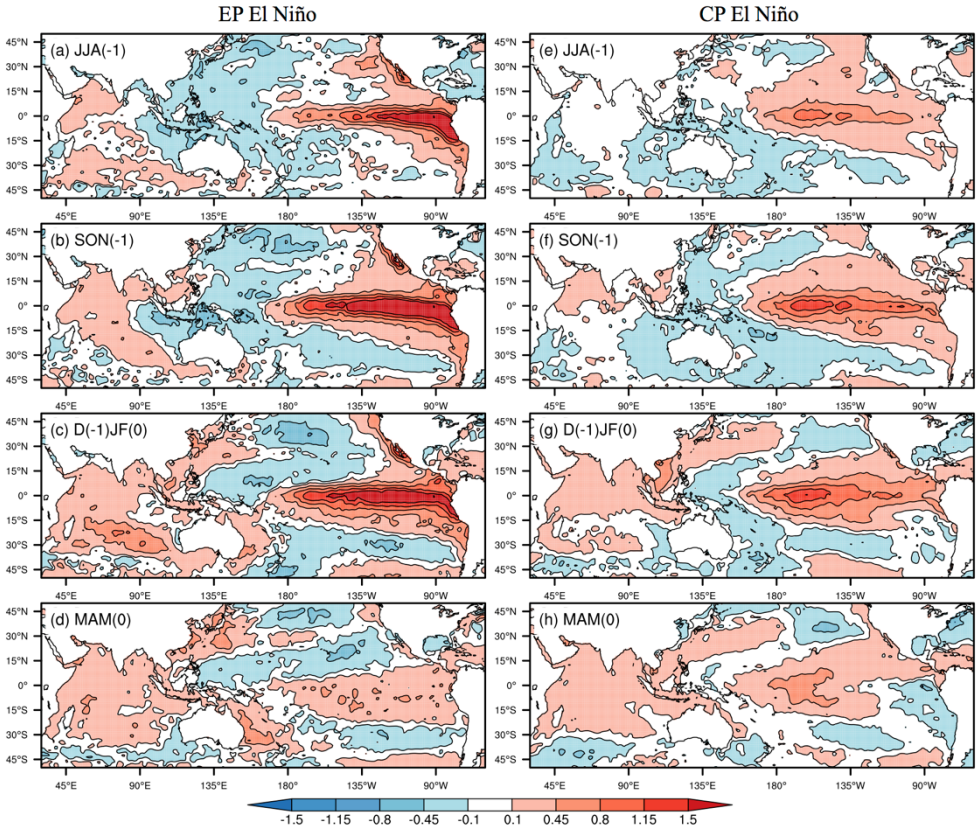

Figure S2 Seasonal evolutions of sea surface temperature anomaly (SSTA) during the EP and CP El Niño event. (a–d) composite SSTA evolution in EP El Niño, (e–h) composite SSTA evolution in CP El Niño.

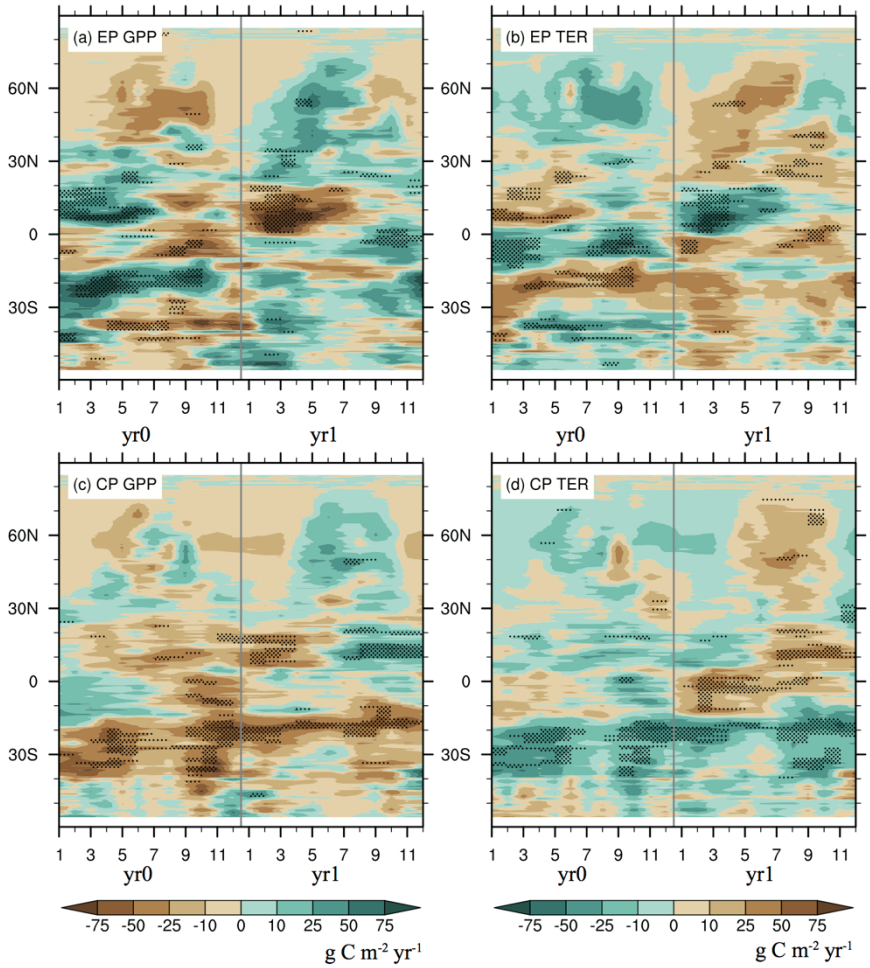

Figure S3 Hovmöller diagrams of the anomalies of terrestrial GPP and TER (averaged from 180°W to 180°E) during two types of El Niños. (a and c) GPP anomaly during EP and CP El Niño events, (b and d) TER anomaly during EP and CP El Niño events. Dotted areas indicate the significance above the 80% level estimated by Student's *t*-test.

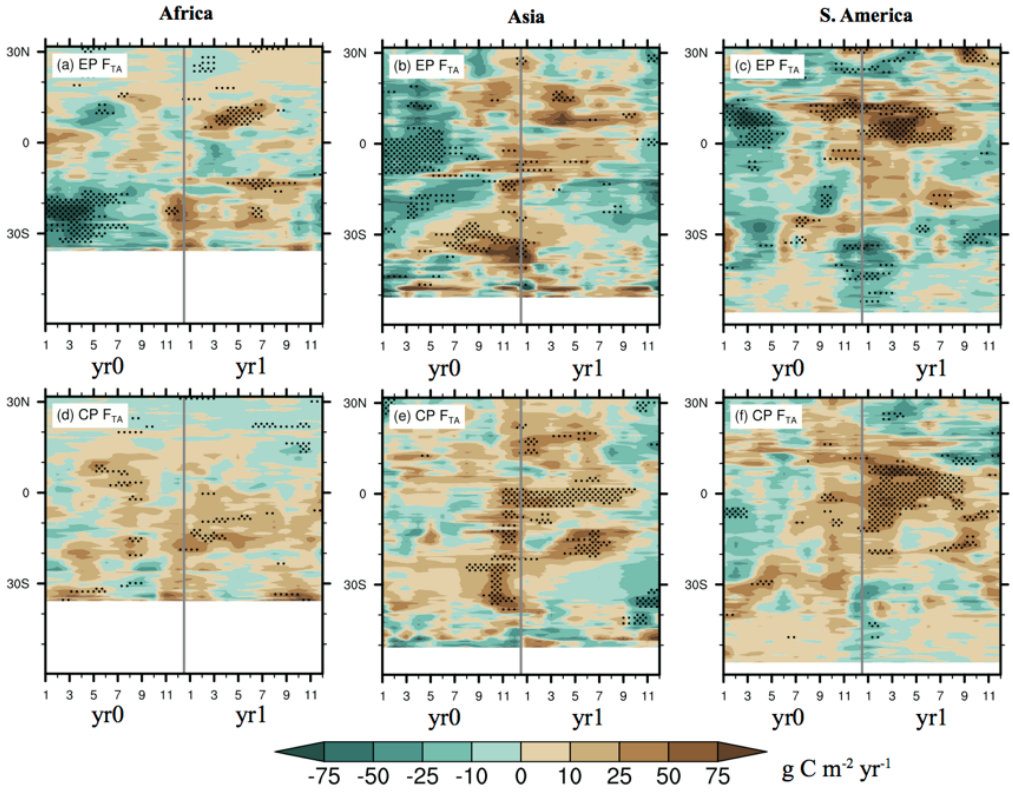

Figure S4 Hovmöller diagrams of the anomalies of F_{TA} during two types of El Niños. (a and d) F_{TA} anomaly over the Africa during EP and CP El Niños; (b and e) F_{TA} anomaly over the Asia during EP and CP El Niños; (c and f) F_{TA} anomaly over the South America. Dotted areas indicate the significance above the 80% level estimated by Student's *t*-test.

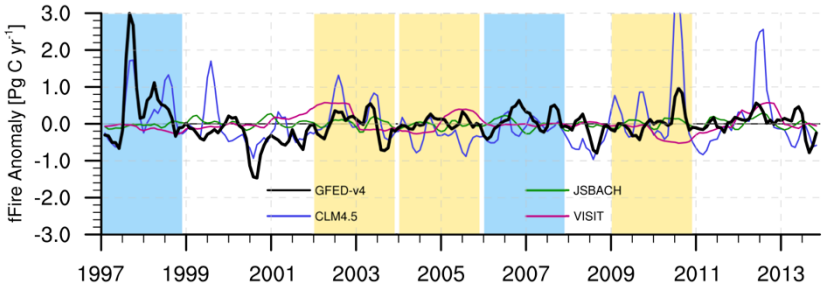

Figure S5 Carbon flux anomalies caused by wildfires from 1997 to 2013. The bars represent the El Niño events during this period selected in this study, with the EP El Niño in blue and CP El Niño in yellow. The GFED-v4 dataset can be referred to Randerson et al. (2015).

Reference

Randerson, J. T., van der Werf, G. R., Giglio, L., Collatz, G. J., and Kasibhatla, P. S.: Global Fire Emissions Database, Ver- sion 4 (GFEDv4), ORNL DAAC, Oak Ridge, Tennessee, USA, https://doi.org/10.3334/ORNLDAAC/1293, 2015.